



Contents lists available at ScienceDirect

Optics Communications

journal homepage: www.elsevier.com/locate/optcom

One-dimensional wavelength multiplexed microscope without objective lens

Ariel Schwarz^a, Aryeh Weiss^a, Dror Fixler^a, Zeev Zalevsky^{a,*}, Vicente Micó^b, Javier García^b^a School of Engineering, Bar-Ilan University, Ramat-Gan 52900, Israel^b Departamento de Óptica, Universitat de València, C/Dr. Moliner 50, 46100 Burjassot, Spain

ARTICLE INFO

Article history:

Received 26 October 2008

Received in revised form 7 April 2009

Accepted 8 April 2009

ABSTRACT

A new approach aimed to achieve microscopic imaging without objective lenses and based on wavelength multiplexing of the spatial object information is presented. The proposed method is used to develop, construct and experimentally validate a new type of optical microscope having no objective lens and no numerical reconstruction algorithms to allow imaging process. In order to extract the collected spatial information we use a spectrometer as part of our microscope system. Preliminary results are presented while considering two different types of one-dimensional (1-D) objects.

© 2009 Elsevier B.V. All rights reserved.

1. Introduction

Microscopy without lenses (or lens-less microscopy) starts as early as in 1948 when Dennis Gabor proposed a new principle to achieve imaging in microscopy working without lenses [1]. Gabor's work was aimed to overcome the limitations of lenses, particularly those of electric and magnetic lenses in electron microscopy. In-line holography with spherical waves, as originally proposed by Gabor, is the simplest realization of the holographic method, working without lenses. Some years later, Leith and Upatnieks applied the Gabor's concept to the optical region [2–4]. Nowadays, recent developments in solid-state image sensors and digital computers have enabled in-line holography as a real powerful tool where 3-D imaging with micrometer resolution [5,6] and tracking moving objects [7–9] has been achieved successfully. Although the recovery of the complex amplitude distribution is inherent to holography, digital in-line holography needs time consuming numerical reconstruction algorithms in order to achieve optical imaging [5,10].

On the other hand, wavelength multiplexing is a widespread and effective approach mainly applied to network communications and fiber optic data transmission [11]. However, many other applications such as optical encryption [12,13], 2-D optical wavelet analysis [14,15], pattern recognition [16–18], image transmission through optical fiber [19–22], optical super resolution [23–27] and so on are benefited from wavelength multiplexing approaches. Basically, the underlying principle of a wavelength multiplexing approach is based on the use of a dispersive optical element such as a grating or a prism to spread a broadband illumination source into single components in such a way that the input object is spatially painted with different wavelength. This fact can be under-

stood as a process in which the spatial object information is encoded into spectral information. After being imaged or transmitted to a limited spatial bandwidth channel, the input object information is recovered by using a similar decoding system to that one used in the encoding stage.

Recently, the concept of wavelength multiplexing has been extended to broadband illumination and applied to several disciplines demonstrating different imaging capabilities. Thus, miniaturized endoscopes for medical 3-D applications [28,29], optical coherence tomographic imaging [30–32], digital holographic applications [33–35], and spectrally confocal microscopes [36,37] have been proposed during the last years as useful methods having real practical implementations. Other relevant lens-less microscopic systems were previously reported in Ref. [6] and 3D microscopy by wavelength multiplexing with a spectrometer was recently reported in Ref. [38].

In this paper, we present a method based upon wavelength coding that is used to test the capabilities of a new type of optical microscope having no objective lenses and no need of digital propagation algorithmic to perform imaging. Instead of both an imaging system (typically a microscope objective and a tube lens) and a detector (typically a CCD), we only use a spectrometer as main part of our microscopic system in order to translate the wavelength coded information into the reconstructed spatial distribution. Since normally spectrometer also contains a CCD as the detector (as well as grating or some other optical elements) the proposed system may also produce the required digital output that is representing the imaged object.

The basic concept of this paper includes experimental demonstration of 1-D wavelength coding. However, although the proposed microscope configuration does not have an objective lens, it still needs a good quality condenser in the illumination stage. Thus, in strict way, the proposed configuration is not completely a lens-less setup.

* Corresponding author. Tel.: +972 3 5317055; fax: +972 3 7384051.
E-mail address: zalevsky@eng.biu.ac.il (Z. Zalevsky).

But the proposed approach gains four possible advantages over conventional microscopic configuration. First of all, the wavelength coding can allow the definition of larger magnification (optical zooming) without payment in the field of view because the different colors used for the wavelength coding can actually code the field of view while applying the maximal required magnification.

Second, if in addition to the lateral coding each wavelength is focused in a different axial distance, one can achieve extension in depth of focus while each axial distance is coded with different wavelength. Therefore, in the decoding stage, the information coming from different axial locations can also be separated by the spectrometer.

Third, the fact that the different wavelengths are spatially spread means that the chromatic performance required from the condenser lens is reduced. In our case we want to have chromatic aberrations rather than design a lens that reduces them.

And finally, because the spatial information is converted or coded into spectral information, it may be coupled into a fiber and transmitted to another location where the spectrometer may decode the coded information and to reconstruct the image [26]. Therefore, the microscope does not have to be a single unit and may be a distributed device which may assist in some biomedical measurements where it is problematic to allocate the analysis equipment in the surgery room where the sample is.

The paper is constructed as follows. In Section 2 we discuss our approach from a qualitative point of view while a theoretical system analysis is presented in Section 3. In Section 4 we present 1-D preliminary experimental results, which are finally discussed in Section 5.

2. System description

The optical setup for the wavelength multiplexing microscope is depicted in Fig. 1 and can be described as follows. A white light source is used to provide broadband illumination at the experimental setup. The illumination light is focused by a condenser lens at the input plane. But, in this optical path, we inserted a diffractive optical element (DOE) to provide spectral separation of the different monochromatic components that integrate the white light illumination. Thus, the spectrum is dispersed by the DOE in such a way that every position at the spatial region of interest in the sample plane is covered with different wavelengths. The zero order beam path is blocked by a screen. Note that the DOE can be positioned at any position between the condenser and the object plane. Shifting the DOE will change the spatial scaling of the colors spreading.

After spreading, the color spectral distribution illuminates the object pattern that is placed in the first diffraction order of the DOE in such a way that different ranges of wavelengths ($\Delta\lambda$) illuminate different pixels of the object. Thus, all the spatial information of the object is encoded by different wavelength distributions. After that, the light is collected into spatial single position and therefore the spatial information is lost. However, the decoding is possible since the amplitude of every wavelength is proportional to the spatial transmission of the specific pixel of the object pattern that was coded with a given wavelength. The light that is collected into a single spatial pixel is analyzed with spectrometer that is connected to the microscopic system. The spectrometer decodes the encoded spatial information and provides high spatial imaging res-

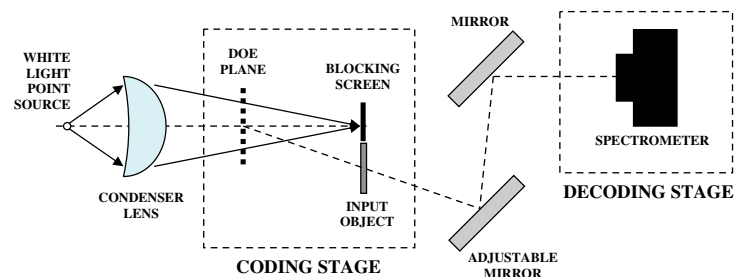


Fig. 1. Schematic of the experimental setup.

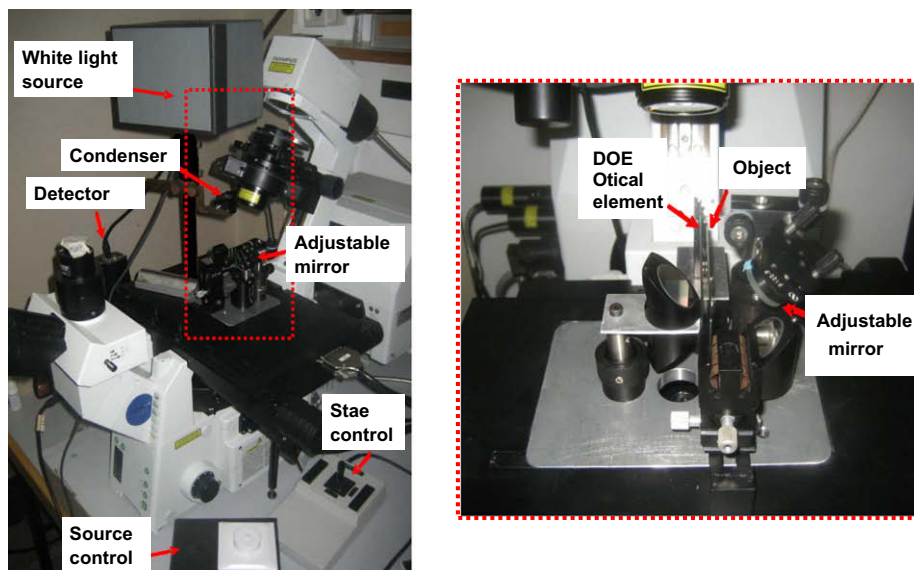


Fig. 2. Images of the constructed microscopic system: whole system (left) and magnified image of the input plane (right).

olution although no objective lenses were used in the microscope itself. After the decoding, the axis of the spectral analysis is proportional to the spatial axis of the reconstructed object. Fig. 2 shows the experimental setup that was constructed at the laboratory where the main body of a commercial microscope was modified to allocate the new components of the proposed approach.

As DOE element in the experiments, we use a 1-D diffraction grating (150 lp/mm). This fact does not imply a lack of generality because a more general 2-D DOE can be used for two-dimensionally spreading the light into different colors. Moreover, such 2-D spectral coding will allow 2-D imaging if a 2-D spectrometer is also used in the decoding stage. An example for an optical element that may perform the 2-D spectral coding may be even a zone plate that can be used instead of, or in addition to, the condenser. The focal length of a zone plate is inversely proportional to the wavelength. Thus, longer wavelengths will have shorter focal length. Thus, in a given plane where the object is positioned one will have a set of rings each having different spectral content since the defocusing of each wavelength, in that plane, is different. The central spot will be white and as one goes away from the center the color will become more and more monochromatic. Although in this case it is not correct to say that every spatial position in the object plane is illuminated by a different wavelength, what we do have in this case is that every spatial position is illuminated by a mixture of colors with different spectral range and this is also enough to obtain the desired decoding of the spatial information (the coordinate transformation matrix relating colors with space is not diagonal in this case but nevertheless it is invertible). Another option can of course be the 2-D grating like element that is described in Ref. [26]. However, in this paper we only present preliminary results for 1-D objects although 2-D samples will be analyzed in an upcoming paper. For this reason, we maintain DOE notation instead of 1-D grating along the paper.

Thus, white light incoming from a halogen source is projected onto a 1-D grating in order to disperse the broadband illumination into its spectral components of different wavelengths. This chromatically dispersed beam is spread over the input object by taking the spectral distribution provided at the first diffraction order of the 1-D grating. Special mechanical holders were designed for both the grating and the object, in order to control the distance between them. A set of reflective mirrors allow that the object transmitted distribution will reach the last component of the system, that is, the spectrometer. In the experiments, we use a 2-D PARISS CCD spectral system (Lightform, Inc, Hillsborough NJ, USA) having a spectral resolution of $\Delta\lambda = 1$ nm.

3. System analysis

The proposed approach is 1-D analyzed using the simplified configuration appearing in Fig. 3. The white light point source is focused at the input plane after passing through a 1-D DOE element.

The field distribution right after the DOE is composed by three terms. The first term denotes the spectrum of the illuminating source, the second one is the converging spherical wave represen-

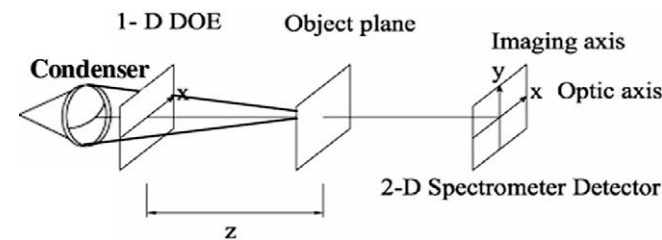


Fig. 3. A simplified version of the optical setup.

tative of the condenser lens, and the last one is the effect of the DOE (first diffraction order of the 1-D grating) which is wavelength dependent. Mathematically, we obtain

$$u_{DOE}(x_{DOE}, \lambda) = S(\lambda) \exp\left(\frac{-\pi i}{\lambda z} x_{DOE}^2\right) \exp\left(\frac{2\pi i \lambda}{\lambda} x_{DOE}\right) \quad (1)$$

being d the period of the DOE, x_{DOE} the coordinate in the DOE plane, λ the optical wavelength, u_{DOE} is the field distribution in the DOE plane, and $S(\lambda)$ the spectral distribution of the white light point source. Notice that we have only considered one of the diffraction orders of the grating because we are interested in the spectral dispersion provided by such element (other diffraction orders are blocked by a screen).

After that, such field distribution propagates in free space a distance of Z until it reaches the object plane. The field distribution that is obtained in that plane is

$$u_{obj.}(x_{obj.}, \lambda) = \exp\left(\frac{i\pi}{\lambda Z} x_{obj.}^2\right) \int u_{DOE}(x_{DOE}, \lambda) \times \exp\left(-\frac{2\pi i}{\lambda Z} x_{obj.} x_{DOE}\right) \exp\left(\frac{\pi i}{\lambda Z} x_{DOE}^2\right) dx_{DOE} \quad (2)$$

where $u_{obj.}$ is the field distribution in the object plane, $x_{obj.}$ is the spatial coordinate of this plane and Z is the free space propagation distance designated in Fig. 3.

Neglecting constant factors, substituting Eq. (1) into Eq. (2) and carrying out some mathematical simplifications yields

$$u_{obj.}(x_{obj.}, \lambda) = S(\lambda) \exp\left(\frac{i\pi}{\lambda Z} x_{obj.}^2\right) \int \exp\left[\frac{2\pi i}{\lambda} x_{DOE} \left(\frac{\lambda}{d} - \frac{x_{obj.}}{Z}\right)\right] dx_{DOE} \quad (3)$$

Solving the integral, we obtain the field distribution just in a plane before the input object

$$u_{obj.}(x_{obj.}, \lambda) = S(\lambda) \exp\left(\frac{i\pi}{\lambda Z} x_{obj.}^2\right) \delta\left(x_{obj.} - \frac{\lambda Z}{d}\right) = S(\lambda) \exp\left(\frac{i\pi \lambda Z}{d^2}\right) \delta\left(x_{obj.} - \frac{\lambda Z}{d}\right) \quad (4)$$

When multiplied by the object pattern $g(x_{obj.})$, the obtained result is

$$u_{obj.}(x_{obj.}, \lambda) = g(x_{obj.}) S(\lambda) \delta\left(x_{obj.} - \frac{\lambda Z}{d}\right) \quad (5)$$

Note that we have neglected a constant phase factor. The δ function in Eq. (5) selects the location of the beams where $x_{obj.} = z\lambda/d$ and the spatial location of every pixel Δx is determined by the spectral resolution $\Delta\lambda$

$$\Delta x_{obj.} = \frac{z\Delta\lambda}{d} \quad (6)$$

Therefore the spatial resolution Δx is determined by the spectral resolution $\Delta\lambda$.

Note that the result of Eq. (4) is a theoretical one. In practice the focusing spot on the object plane (without the DOE) that is generated by the condenser is diffraction limited. Assuming that the diameter of the condenser lens is D , and that $z = F$ (F is the focal length of the condenser) in that case the integrals of Eq. (3) are finite and therefore Eq. (4) is becoming to be

$$u_{obj.}(x_{obj.}, \lambda) = S(\lambda) \exp\left(\frac{i\pi \lambda F}{d^2}\right) \text{sinc}\left(\frac{D}{d} - \frac{D x_{obj.}}{\lambda F}\right) \quad (7)$$

Thus the spatial resolution limit δ_{res} is bounded by

$$\delta_{res} = \frac{\lambda F}{D} \quad (8)$$

that is, by the width of the sinc function. Therefore D will also limit the resolution of the system in addition to the spectral resolution of the spectrometer.

4. Experimental results

Two different objects are used in order to demonstrate the principle of operation of the system: a grating (periodic object) and a bar-code (non-periodic object). Since the spatial resolution is related to the spectral resolution of the spectrometer as well as the spectral bandwidth of the white light source (see Eq. (6)), we first measured the spectrum of the source (halogen lamp). The result is presented in Fig. 4. The period of the grating that we used in order to disperse the colors is $d = 6.67 \mu\text{m}$.

Note that the illumination source presented in Fig. 4 also passed through the spectral filter of the microscope. In principle instead of using the halogen lamp as we did, one may combine several light sources (and to remove the filter of the microscope) in order to have wider spectral bandwidth to make better usage of the sensitivity bandwidth of the spectrometer (it has some sensitivity even at wavelengths close to 1000 nm).

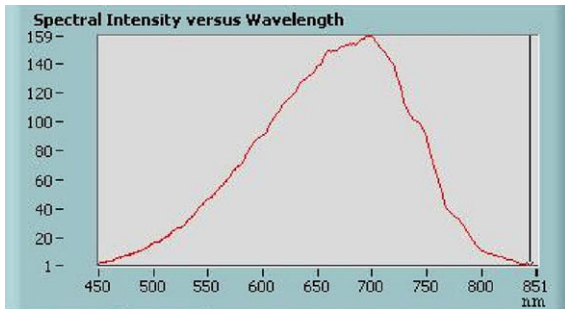


Fig. 4. Spectral mapping of the halogen lamp source.

4.1. Periodic object: grating pattern

The object grating which was imaged is shown in Fig. 5a. Its dimensions were about $0.5 \text{ mm} \times 1 \text{ mm}$, and its spatial frequency was 10 lp/mm ($\Delta x = 100 \mu\text{m}$). The bandwidth of the system in this example was chosen to be 110 nm approximately (from 540 to 650 nm).

The system was calibrated according with the following procedure. First we imaged the first diffraction order of the linear spectral separation (i.e. the position of each wavelength after dispersion which is proportional to the wavelength itself) into the spectrometer. In other words, we performed a measurement without the object (Fig. 5a). This measurement is important in order to analyze the changes in the wavelengths intensity caused by the object that will be inserted into the setup later on. In the second step, the object was inserted into the system and imaged. After the decoding done by the CCD spectrometer, we obtained the result seen in Fig. 5b. Those results were normalized by the spectrum of the illumination source. The normalized results are shown in Fig. 5c (lower part) where one may see the reconstructed grating pattern. One may see that the reconstructed image and the real structure of the grating object do indeed match. Moreover, the third black bar presented in the lower part of Fig. 5c is deeper than the other two as it also corresponds with Fig. 5b. This is due to the halogen lamp spectrum which is more intense in the reds than in the blues.

The free space distance that was generated in the setup was $z = 2.6 \text{ mm}$. Eq. (6) shows that for $z = 2.6 \text{ mm}$, $d = 6.67 \mu\text{m}$ and $\Delta x = 100 \mu\text{m}$, the period of the grating of the object should be with $\Delta \lambda = 25 \text{ nm}$ which is exactly the period as it is seen in Fig. 5c.

Note that the experimentally achieved field of view was approximately 0.44 mm. Since in this field of view we sampled about 110 spatial points, this yields spatial resolution of $4 \mu\text{m}$

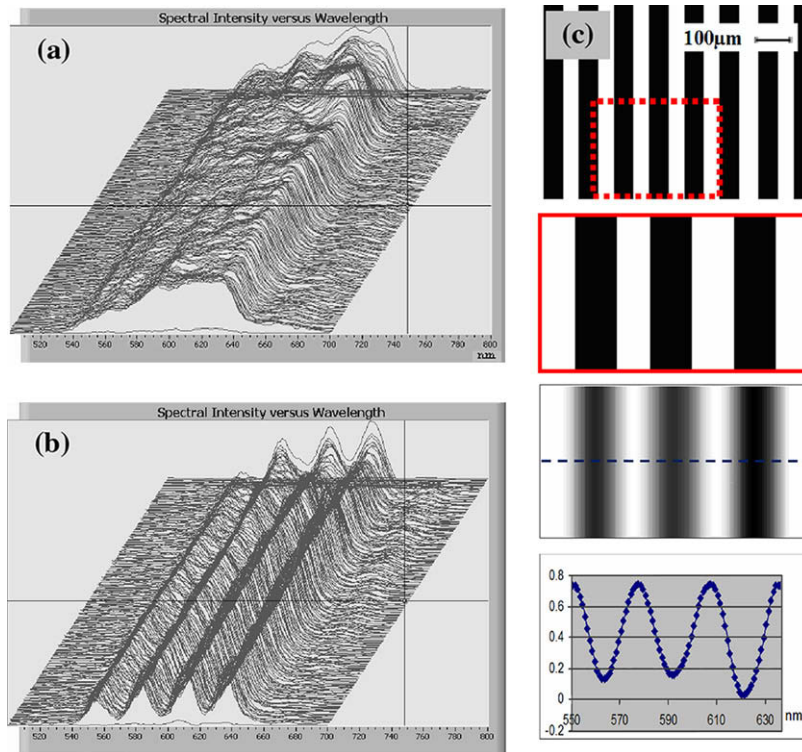


Fig. 5. First order results without the object. (b): Spectral intensity of the reconstruction results, obtained at first diffraction order, with the grating pattern. (c): from up to down, the grating pattern used for the experiment, a magnified area of the grating pattern with the same dimensions than the presented measured results, the normalized result of (b), and a plot of the measured reconstructed grating (cross section along the dashed blue line). (For interpretation of the references in colour in this figure legend, the reader is referred to the web version of this article.)

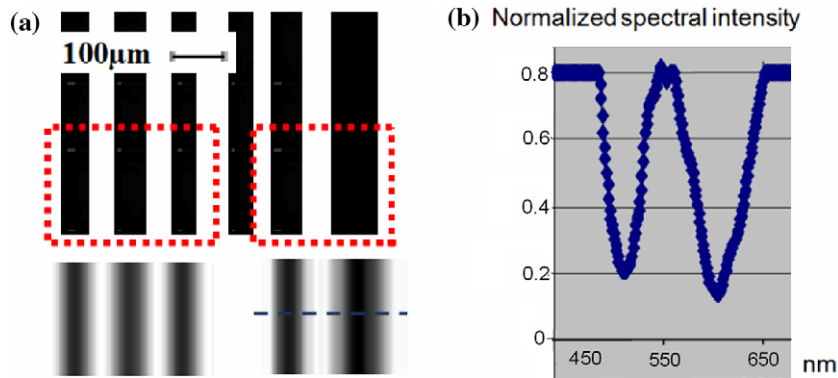


Fig. 6. (a): Barcode pattern used for the experiment: the original barcode (upper part) and its reconstruction images using the proposed system (lower part). (b): Normalized spectral intensity plot section along the blue dashed line in one of the reconstructed images.

which for central wavelength of 500 nm yields an equivalent F-number of 8 and an equivalent numerical aperture of 0.0625.

4.2. Non-periodic object: barcode pattern

The barcode pattern used in the experiment is shown in the upper part of Fig. 6a while in the lower part of the same figure, we present the normalized outputs of the spectrometer after being normalized by the spectral distribution of the white light source and corresponding with the marked dot red line rectangles of the upper part. Fig. 6b represents a plot section along the dashed blue line of one of the reconstructed images. Once again, the black vertical bar corresponding with the red spectral region of the white illumination is deeper than the other one as it corresponds with a higher intensity of the light source in this spectral region. Also, the spectral periodicity that was measured in Fig. 6b is again approximately 25 nm.

4.3. Biological object: brain section

The object in this sample was a brain tissue section from a rat (Fig. 7a). The sample included a region of cells surrounded by extracellular space. The border of the cell-containing region is seen in Fig. 7a. The magnified boundary region of the cells was obtained with bright field microscope with a magnification of 100×. The smaller scale image of Fig. 7a was obtained with magnification of 10×.

The tissue samples were frozen in liquid nitrogen and stored at -70°C until extraction. For extraction, the punches were thawed and subjected to probe sonication (80 W for 5 s with a Sonifier B-12; Branson Sonic Power Company, Danbury, CT) in

0.5 ml of a perchlorate solution (0.1 M) containing EDTA/ethanol (0.02/1%) on ice.

In the lens-less microscope we tried to reconstruct the boundary region of the cells without using an objective lens. The reconstructed results obtained after the decoding with the spectrometer, are presented in Fig. 7b. One may see the reconstructed border of the cellular region (the pink region in Fig. 7b). The region presented in Fig. 7b is approximately 80 by 100 μm .

Note that the 2-D experimental results of Fig. 7b were obtained by 1-D wavelength multiplexing as previously described in this manuscript. The information in the second dimension was obtained by scanning with the 1-D spectral distribution and applying the proposed wavelength based imaging approach for different cross sections of the 2-D sample.

5. Discussion and conclusions

In this paper, we have introduced a new type of lens-less microscope in the imaging stage. The purpose of this research was to establish a new microscope principle without objective lenses in which the spatial information of the objects is encoded with optical wavelengths and later on decoded (i.e. analyzed and reconstructed) by a spectrometer that is connected to the microscopic system. The proposed system was built and preliminary 1-D results demonstrated its feasibility. Work is now underway to obtain higher quality 2-D images using the proposed lens-less configuration.

In general, in comparison with previous lens-less microscope architectures, the proposed approach may have two differences. First, the proposed setup is able to perform imaging without any digital post-processing stage involving complex and time consum-

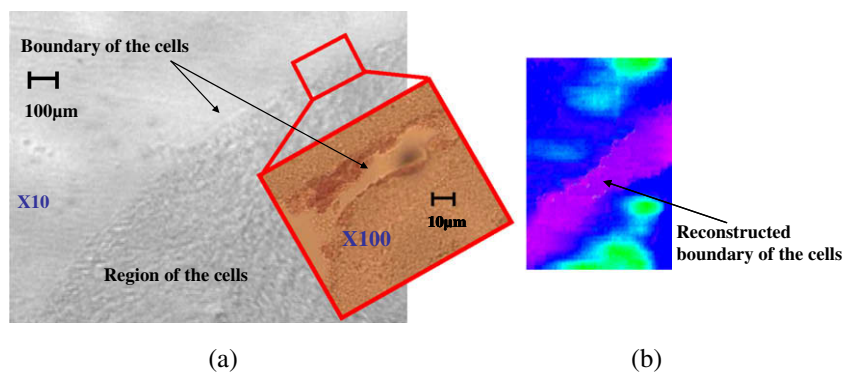


Fig. 7. (a). High resolution image of the biologic object which was plurality of brain cells. (b). Image of the reconstruction obtained for the boundary region of the cells.

ing propagation algorithms. The method only requires an initial calibration stage over the illumination spectral distribution in order to analyze the wavelength intensity changes caused by the object to be imaged. Second, the use of a diffraction grating rather than a prism (as in previous studied wavelength multiplexing approaches) has several advantages such as having larger angular (and therefore spatial) separation between various wavelengths, having linear angular spectrum separation, providing flexibility in the design of the spectral distribution and the overall optical set-up and may produce 2-D wavelength coding (and thus it does not require scanning procedure for the reconstruction of the 2-D image).

As it was stated in the introduction section, the proposed approach may gain four main advantages in comparison to conventional microscope configurations. First (item #1), the wavelength coding may be used to obtain increased magnification without field of view restrictions which will be coded with the wavelengths (and later on decoded). Second (item #2), the wavelength coding can be used to code the axial rather than the lateral axis and by that to obtain increased depth of focus. Third (item #3), due to the wavelength coding the chromatic aberration specifications that are required from the condenser lens are significantly reduced. And forth (item #4), the encoding unit can be separated from the decoding one, which may assist in some real-time surgical operations requiring imaging.

Small clarification regarding item #1: If one increases the magnification of a given system he gains resolution in the object plane since every pixel in the detection array has smaller foot print in the object plane. This increased resolution reduces the field of view, i.e. assuming that one wishes to increase the resolution in the object plane by a factor of three he will reduce the field of view by the same factor. Now returning to our case, if one uses the color coding in order to illuminate the object plane and then to multiplex all colors together he can still have the desired magnification but without resulting in a reduced field of view since the various regions of the field of view that were multiplexed before can now be demultiplexed by the spectrometer (in the demultiplexing process each color will designate a different region in the field of view and one will be able to construct larger overall field of view). In this application instead of coding spatial resolution we are coding the spatial regions of the field of view.

Regarding item #2 the meaning of this was not to use the grating allowing the encoding and decoding of lateral resolution but rather to use an element similar to a zone plate where the wavelengths coding is used to code axial rather than lateral resolution. In a zone plate every wavelength is focused in a different distance and thus analyzing the information collected by the spectrometer may allow one to know from which axial distance the information has arrived. Due to the spectral dispersion the overall depth of focus of the system is extended approximately by:

$$\Delta F = F_0 \cdot \frac{\Delta\lambda}{\lambda_0 - \frac{\Delta\lambda^2}{4\lambda_0}} \quad (9)$$

and this is in addition to the original depth of focus range obtained for every wavelength (proportional to F -number square). In Eq. (9) ΔF is the change in the focal length, F_0 is the focal length for the central wavelength λ_0 while the illuminating spectral bandwidth is from $\lambda_0 - \Delta\lambda/2$ to $\lambda_0 + \Delta\lambda/2$. This implementation will allow imaging thick objects as well as to estimate their 3-D structure and thus it may be very applicable to microscopy.

Note also that the number of spatial degrees of freedom that the spectrometer (which is used in order to decode the spatial information) can resolve equals to the spectral illumination bandwidth divided by its spectral resolution. For instance, if the spectral bandwidth of the illumination is 800 nm (from 400 to 1200 nm) and the

spectrometer resolution is 1 nm, the number of spatial degrees of freedom that can be multiplexed using wavelength coding is 800. But even in case that this number equals only a few hundred of degrees of freedom yet the advantages proposed in item #1 and 2 can be achieved. In item #1 where one may obtain optical zooming without sacrificing the field of view even a zooming factor of $3 \times$ is significant and thus no more than $3 \times 3 = 9$ separable points are required from the spectrometer. In the case of item #2 the extension in the depth of focus even by a factor of 3 is significant and thus here even 3 separable points are sufficient. Obviously since the spectrometer can actually resolve hundreds of points very significant improvement may be obtained in the applications discussed in item #1 and #2.

Although a 1-D diffraction grating acting as DOE is used in the experimental validation of the proposed approach, and thus 1-D imaging is achieved, it is in principle possible to achieve 2-D imaging by performing 1-D scanning over the second dimension (the axis that is perpendicular to the axis at which the colors are spread). In this case, the proposed approach will perform 2-D imaging by using wavelength-time multiplexing of the spatial object information. However, the proposed approach can exhibit 2-D imaging by using a 2-D DOE which spreads the colors distribution over the input plane (as zone plate element that was previously described) and, in that case, the mechanical 1-D scanning may be avoided.

Acknowledgments

Javier García and Vicente Micó acknowledge the support provided to this work by the Spanish Ministerio de Educación y Ciencia under the project FIS2007-60626.

Aryeh Weiss acknowledges the support provided to this work by ISF institutional equipment Grant #1436/05.

Zeev Zalevsky acknowledges the support provided to his work by the Israeli ministry of science, culture and sport by Grant #3-3426.

References

- [1] D. Gabor, *Nature* 161 (1948) 777.
- [2] E.N. Leith, J. Upatnieks, *J. Opt. Soc. Am.* 52 (1962) 1123.
- [3] E.N. Leith, J. Upatnieks, *J. Opt. Soc. Am.* 53 (1963) 1377.
- [4] E.N. Leith, J. Upatnieks, *J. Opt. Soc. Am.* 54 (1964) 1295.
- [5] W. Xu, M.H. Jericho, I.A. Meinertzhagen, H.J. Kreuzer, *Proc. Natl. Acad. Sci. USA* 98 (2001) 11301.
- [6] G. Pedrini, H.J. Tiziani, *Appl. Opt.* 41 (2002) 4489.
- [7] W. Xu, M.H. Jericho, I.A. Meinertzhagen, H.J. Kreuzer, *Opt. Lett.* 28 (2003) 164.
- [8] J. Sheng, E. Malkiel, J. Katz, *Appl. Opt.* 45 (2006) 3893.
- [9] F. Dubois, N. Callens, C. Yourassowsky, M. Hoyos, P. Kurowski, O. Monnom, *Appl. Opt.* 45 (2006) 864.
- [10] L.P. Yaroslavsky, *Digital Holography and Digital Image Processing: Principles, Methods, Algorithms*, Kluwer, 2003.
- [11] B. Mukherjee, *Optical Wavelength Division Multiplexing (WDM) Networks*, Springer, 2006.
- [12] G.H. Situ, J.J. Zhang, *Opt. Lett.* 30 (2005) 1306.
- [13] L. Chen, D. Zhao, *Opt. Express* 14 (2006) 8552.
- [14] J. García, Z. Zalevsky, D. Mendlovic, *Appl. Opt.* 35 (1996) 7019.
- [15] J.J. Esteve-Taboada, J. García, C. Ferreira, D. Mendlovic, Z. Zalevsky, *J. Opt. Soc. Am. A* 18 (2001) 157.
- [16] S.K. Case, *Appl. Opt.* 18 (1979) 1890.
- [17] H.O. Bartelt, *Opt. Commun.* 29 (1979) 37.
- [18] Z. Zalevsky, D. Mendlovic, J. García, *Appl. Opt.* 36 (1997) 1059.
- [19] C.J. Koester, *J. Opt. Soc. Am.* 58 (1968) 63.
- [20] A.A. Friesem, U. Levy, *Opt. Lett.* 2 (1978) 133.
- [21] H.O. Bartelt, *Opt. Commun.* 28 (1979) 45.
- [22] A.M. Tai, A.A. Friesem, *Opt. Lett.* 8 (1983) 57.
- [23] A.I. Kartashev, *Opt. Spectrosc.* 9 (1960) 204.
- [24] J.D. Armitage, A.W. Lohmann, D.P. Paris, *Jpn. J. Appl. Phys.* 4 (1965) 273.
- [25] A.M. Weiner, J.P. Heritage, E.M. Kirschner, *J. Opt. Soc. Am. B* 5 (1988) 1563.
- [26] D. Mendlovic, J. García, Z. Zalevsky, E. Marom, D. Mas, C. Ferreira, A.W. Lohmann, *Appl. Opt.* 36 (1997) 8474.
- [27] J. García, V. Micó, D. Cojoc, Z. Zalevsky, *Appl. Opt.* 47 (2008) 3080.
- [28] G.J. Tearney, M. Shishkov, B.E. Bouma, *Opt. Lett.* 27 (2002) 412.

- [29] D. Yelin, W.M. White, J.T. Motz, S.H. Yun, B.E. Bouma, G.J. Tearney, *Opt. Express* 15 (2007) 2432.
- [30] M. Laubscher, S. Bourquin, L. Froehly, B. Karamata, T. Lasser, *Opt. Commun.* 237 (2004) 275.
- [31] L. Yu, M. Kim, *Opt. Express* 12 (2004) 6632.
- [32] L. Yu, M. Kim, *Opt. Express* 13 (2005) 5621.
- [33] D. Kim, J.W. You, S. Kim, *Opt. Express* 14 (2006) 229.
- [34] J. Kühn, T. Colomb, F. Montfort, F. Charrière, Y. Emery, E. Cuche, P. Marquet, Ch. Depeursinge, *Opt. Express* 15 (2007) 7231.
- [35] Ch.J. Mann, P.R. Bingham, V.C. Paquit, K.W. Tobin, *Opt. Express* 16 (2008) 9753.
- [36] G.J. Tearney, R.H. Webb, B.E. Bouma, *Opt. Lett.* 23 (1998) 1152.
- [37] D. Yelin, C. Boudoux, B.E. Bouma, G.J. Tearney, *Opt. Lett.* 32 (2007) 1102.
- [38] L. Yu, Z. Chen, *Opt. Lett.* 32 (2007) 3005.